Letter

Exact face-landing probabilities for bouncing objects: Edge probability in the coin toss and the three-sided die problem

Lluís Hernández-Navarro [1,4,*] and Jordi Piñero [2,3,4,†]

[1]*Institut d'Investigacions Biomèdiques August Pi i Sunyer (IDIBAPS), Barcelona, Spain*
[2]*ICREA-Complex Systems Laboratory, Universitat Pompeu Fabra, 08003 Barcelona, Spain*
[3]*Institut de Biologia Evolutiva (CSIC-UPF), Psg Maritim Barceloneta, 37, 08003 Barcelona, Spain*
[4]*The Rashevsky Club, Barcelona, Spain*

(Received 27 March 2021; revised 8 January 2022; accepted 24 January 2022; published 17 February 2022)

Have you ever taken a disputed decision by tossing a coin and checking its landing side? This ancestral "heads or tails" practice is still widely used when facing undecided alternatives since it relies on the intuitive fairness of equiprobability. However, it critically disregards an interesting third outcome: the possibility of the coin coming at rest on its edge. Provided this evident yet elusive possibility, previous works have already focused on capturing all three landing probabilities of thick coins, but have only succeeded computationally. Hence, an exact analytical solution for the toss of bouncing objects still remains an open problem due to the strongly nonlinear processes induced at each bounce. In this Letter we combine the classical equations of collisions with a statistical-mechanics approach to derive an exact analytical solution for the outcome probabilities of the toss of a bouncing object, i.e., the coin toss with arbitrarily inelastic bouncing. We validate the theoretical prediction by comparing it to previously reported simulations and experimental data; we discuss the moderate discrepancies arising at the highly inelastic regime; we describe the differences with previous, approximate models; we propose the optimal geometry for the fair cylindrical three-sided die; and we finally discuss the impact of current results within and beyond the coin toss problem.

DOI: 10.1103/PhysRevE.105.L022201

I. INTRODUCTION

Since long ago, a great number of scientists have struggled to solve the problem of the face-landing probabilities in real physical tosses. In the seventeenth century, Galilei, Cardano and Huygens already wrote about the die throw and the coin toss problem [1,2]; and Pascal and de Fermat exchanged letters discussing dice games [3]. But, perhaps, the essence of the problem was best put forward by Newton: "*If a die bee not a regular body but a parallelepipedon or otherwise unequally sided, it may bee found how much one cast is more easily gotten then another*" [4].

More than a century later, Simpson [5] suggested a model in which the outcome probabilities were proportional to the solid angle of each face. As such, this model only captured the outcome of a perfectly nonbouncing toss.

Simpson's model has been experimentally rejected for more realistic tosses as reported by Buden [6], Singmaster [7], and Heilbronner [8], yet it is still adopted in current scientific outreach [9] and in recent studies due to its simplicity [10]. Extended versions take into account constraints in the angular momentum [11–14] but still provide a solution for the nonbouncing toss only.

Beyond Simpson's geometrical approach and its extensions, two new classes of models have arisen in the past decades to assess realistic bouncy tosses. On one hand, some studies suggested probabilistic models grounded on the chaotic properties of the coin toss [11,15] as well as phenomenological models based on the Gibbs distribution from equilibrium thermodynamics [16] or on Markovian processes with heuristic transition rates [17,18]. On the other hand, dynamical models grounded on the equations of partially inelastic collisions [19–21] have also been proposed.

As for the latter, a computational model has successfully captured outcome probabilities of partially inelastic bouncing tosses of short cylinders, i.e., coins [19]. Yet, an exact analytical solution has only been found at most for up to two bounces [20].

Of note, coin tossing contributions are not only relevant due to the originality and intrinsic interest of the topic but are also known to entail a well-established impact on a widespread range of cutting-edge physics research fields [12,15].

Here we present the first exact solution of the toss of a bouncing object (i.e., the coin toss with arbitrarily inelastic bouncing) grounded on the equations of collisions from classical mechanics [19], and tackled by means of nonequilibrium statistical mechanics under *a priori* equiprobability of phase states. The latter is simply achieved by highly random initial linear and angular velocities in the toss, and/or by the randomization of these variables after enough partially inelastic collisions take place. The final analytical expression is provided and validated from reanalyzed experimental and numerical data; the specific case of the fair three-sided

*lluishn@gmail.com
†jpinerfe@gmail.com

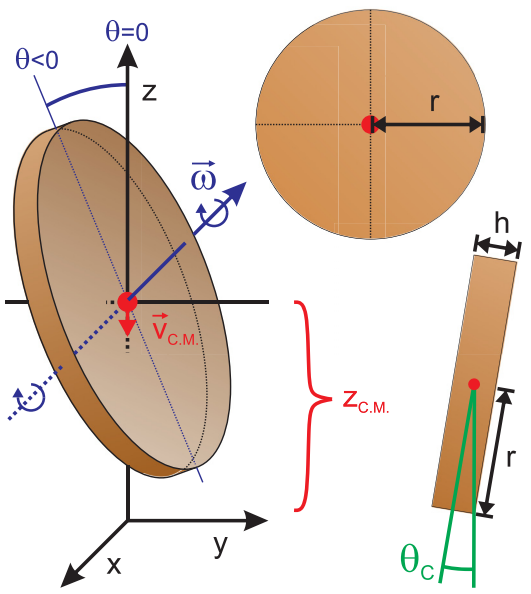

FIG. 1. Coin sketch. The coin, a homogeneous and incompressible cylinder of radius r and height h, is tossed with an initial c.m. height $z\hat{a}_z$ and with vertical velocity $v\hat{a}_z$. The coin's initial orientation with respect to the z axis is depicted by the polar angle $\theta\hat{a}_\theta$ with related angular velocity $-\omega\hat{a}_x$, and the dynamics are fully captured by $\{z, v; \theta, \omega\}$ alone. The *critical angle* θ_c corresponds to the maximum polar angle at which the coin does not tip over its edge.

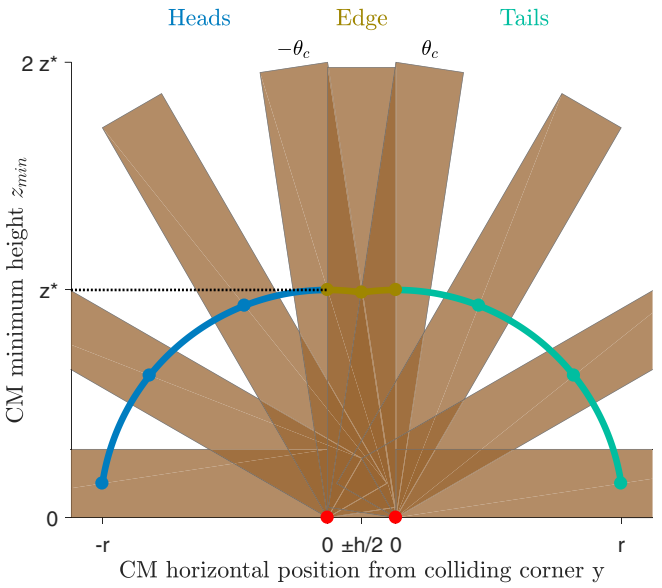

FIG. 2. Minimum potential energy. The minimum potential is proportional to the height of the c.m. when, at least, one of the corners of the coin is in contact with the ground and is set by angle θ as depicted by the solid line. Solid circles on the line depict the position of the c.m. for each instance of the polar angle. Different colors (shades in gray scale) show the instantaneous outcome of the toss, set by the domain of the current θ. When the mechanical energy is lower than the critical value ($E < E_c = mgz^*$), the coin cannot overcome the potential energy at all angles, the angle domains become disjoint, and the final outcome of the toss is bound to its current instantaneous value. Red circles on the x axis depict the coin-ground contact points, i.e., the colliding corners.

cylindrical die is considered; and the implications of the current results within and beyond the coin toss problem are discussed.

II. EXACT MODEL

A. Initial assumptions and approach

The coin is conceptualized as a perfect incompressible cylinder of radius r and height h (Fig. 1). The tossing imbues a linear velocity $\vec{v}$ and an angular speed $\vec{\omega}$ to the coin such that the first vector is purely vertical, and the latter vector is applied to a rotational axis that crosses the coin's center of mass (c.m.) on its diameter parallel to the floor (x axis). The angle of the coin around the x axis is depicted by $\theta(t)$. The coin bounces multiple times on the floor in successive inelastic collisions (characterized by a constant coefficient of restitution γ) with a given dissipation of energy at each bounce and with neglected air and ground frictions. States in the phase space are assumed to be independent of the initial conditions as long as enough bounces take place [15,21]. Hence, we may consider equiprobability of states in the phase space.

B. Model derivation

1. Potential, kinetic, and minimum potential energy

The potential energy U is directly determined by the vertical height z of the c.m. of the coin as $U = mgz$, where m is the mass of the coin, and g is the acceleration of gravity. The kinetic energy corresponds to

$$T = \frac{mv^2}{2} + \frac{I\omega^2}{2}, \tag{1}$$

where I is the moment of inertia of the coin around the rotational axis described previously.

It will be useful to define the minimum potential energy $U_{\min}(\theta) = mgz_{\min}(\theta)$ as the profile of the potential energy depending on θ when, at least, one corner of the coin is in contact with the floor (Fig. 2). Under the previous constraint, the height of the c.m. reads

$$z_{\min}(\theta) = z^* \cos(|\theta| - \theta_c), \tag{2}$$

where $z^* = \sqrt{r^2 + (h/2)^2}$ is the semidiagonal of the coin's cross section, and $\theta_c \equiv \arctan(\frac{h}{2r})$ is the critical angle of the coin (see Figs. 1 and 2).

2. Critical energy

In a coin toss, the system dissipates energy at each collision up to the final (meta)stable state. We define the critical energy E_c as the energy threshold below which the coin is not able to overcome the potential energy barrier that separates its now disjoint θ domains so that the final outcome of the toss is already determined. The critical energy E_c is directly set by the maximum potential energy of the coin when it is in contact

with the floor,

$$E_c = mgz^*. \tag{3}$$

3. Critical collision

We define the *critical collision* as the single collision at which the energy of the coin becomes lower than E_c (as linear and angular velocities are then small, air friction can be neglected). Since angle θ does not change during instantaneous collisions, its value in the immediately prior state to the critical collision already determines the final outcome of the toss.

The states immediately prior to the critical collision are constrained by Eq. (2), i.e., a physical contact between the coin and the floor, and the distribution of states is governed by the equations of partially inelastic collisions.

4. Partially inelastic collision

Partially inelastic collisions are characterized by the change in the vertical velocity of the coin's colliding corner u', that becomes $u'' = -\gamma u'$ after the collision with γ as the constant restitution coefficient. The vertical velocity of the colliding corner fulfills $u = v + y(\theta)\omega$, where v is the c.m.'s vertical velocity, ω is the angular velocity, and y depicts the horizontal position of the coin's c.m. with respect to the colliding corner (see Fig. 2). The angular momentum is conserved when considering a shifted rotational axis that crosses the contact point between the floor and the coin, providing $I\,\Delta\omega = my\,\Delta v$.

By combining these constraints, we obtain the expressions for the changes in the velocity of the c.m., the angular velocity, and the kinetic energy,

$$\Delta v = -(1+\gamma)\frac{I}{I+my^2}(v' + y\omega'), \tag{4}$$

$$\Delta\omega = -(1+\gamma)\frac{my}{I+my^2}(v' + y\omega'), \tag{5}$$

and

$$\Delta E = -\frac{1-\gamma^2}{2}\frac{mI}{I+my^2}(v' + y\omega')^2. \tag{6}$$

These results are consistent with the reduced equations used in the computational study of Ref. [19]. Also in that study it is shown that, whereas the coin may exhibit a "chattering" regime (a regime with very high, increasing bouncing frequency), this transient behavior does not yield a significant energy loss and, thus, does not contribute to critical collisions.

5. Phase space density of prior states

By definition, states immediately prior to the critical collision must have a mechanical energy such that $E'(\theta, v, \omega) \geqslant E_c$, whereas their energy immediately after the collision has to fulfill $E''(\theta, v, \omega) < E_c$ with $E'' = E' + \Delta E$ following Eq. (6). Note that, prior to the collision, the vertical velocity of the coin's colliding corner has to be negative $u' < 0$.

The first condition provides an inequality relating v' and ω' with an active constraint (case "=") that, regarding Eqs. (1)–(3), follows the elliptic surface:

$$\left[\frac{1}{2g(z^* - z_{\min})}\right]v^2 + \left[\frac{I}{2mg(z^* - z_{\min})}\right]\omega^2 \geqslant 1. \tag{7}$$

The second condition introduces an inequality with a constraint surface that follows the tilted ellipse:

$$\left[\frac{I\gamma^2 + my^2}{2g(I+my^2)(z^* - z_{\min})}\right]v^2 + \left[\frac{Iy^2\gamma^2 + I^2/m}{2g(I+my^2)(z^* - z_{\min})}\right]\omega^2 + \left[\frac{Iy(1-\gamma^2)}{-g(I+my^2)(z^* - z_{\min})}\right]v\omega < 1. \tag{8}$$

And the third condition enforces $v + y\omega < 0$.

To derive the density function of prior states ρ depending on θ, we integrate the prior phase subspace over all possible values of the linear and angular momenta $p = mv$ and $L = I\omega$, just before the critical collision. Note that because we are directly integrating the constrained two-dimensional (2D) volume of this subspace, we are implicitly assuming equiprobability of prior states, as discussed in Sec. II A.

As shown in Fig. 3, the aforementioned integration is equivalent to computing the area delimited by the tilted ellipse of Eq. (8), subtracting the area delimited by the ellipse of the complementary of Eq. (7), and halving the result to capture $u' < 0$. Hence, we take into account all prior states at fixed θ that will have less energy than E_c after the collision and discard those that already have below-critical energy.

A general ellipse of the form $AX^2 + BY^2 + CXY = 1$ encloses a total area $S = 2\pi/\sqrt{4AB - C^2}$. Hence, after some algebra, the density function of prior states ρ in terms of θ becomes

$$\rho(\theta) = \frac{\pi m^{3/2} g\sqrt{I}}{h^2}\frac{1-\gamma}{\gamma}[z^* - z_{\min}(\theta)], \tag{9}$$

where h^2 is the phase space volume occupied by a single state and the variable $y(\theta)$ is canceled out such that θ only contributes through $z_{\min}(\theta)$ as in Eq. (2). A multiplicative prefactor mI/h^2 has been introduced in order to properly normalize the phase space (composed of two pairs of conjugated variables: $\{z, p = mv\}$ and $\{\theta, L = I\omega\}$). However, note that this factor cancels out during the computation of the outcome probabilities in the next section.

6. Edge landing probability

The probability of a coin toss landing on edge can be derived as the fraction of prior states in the phase space whose angle θ fulfills $-\theta_c \leqslant \theta \leqslant \theta_c$ (see Fig. 2). Due to coin's symmetry, we can collapse the whole θ domain to the first quadrant, which yields

$$P_E = \frac{\int_{\theta=0}^{\theta=\theta_c}\rho(\theta)d\theta}{\int_{\theta=0}^{\theta=\pi/2}\rho(\theta)d\theta} = \frac{\theta_c - \sin(\theta_c)}{\pi/2 - [\sin(\theta_c) + \cos(\theta_c)]}, \tag{10}$$

that, interestingly, only depends on the geometry of the coin (i.e., θ_c), and not on the restitution coefficient γ. For the examples of 1 £, 1 €, and a quarter \$ coins, the theory predicts an edge outcome probability of 1 over ~1000, 3000, and 8000 tosses, respectively.

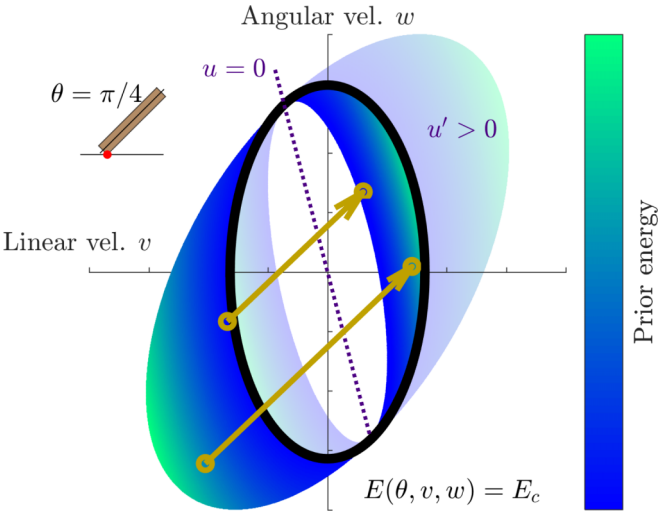

FIG. 3. Phase space prior and posterior to critical collisions. Phase space in v and ω coordinates for an example collision angle ($\theta = \pi/4$), coin geometry ($\theta_c = \pi/6$), and coefficient of restitution ($\gamma = 0.5$) during a (critical) collision. Elliptical black circumference illustrates the critical energy boundary of Eq. (7). The dashed purple line shows the limiting case $u = 0$. The filled solid area encircled between the outer tilted ellipse of Eq. (8) and E_c depicts all the *prior states* that fulfill $u' < 0$ and will become subcritical after a critical collision; the transparent area illustrates nonphysical $u' > 0$. The filled solid surface composed between E_c and the inner tilted ellipse encloses all the phase states that are possible immediately after a critical collision; the transparent surface depicts nonphysical $u'' < 0$. The inner tilted ellipse is obtained by reversing time with $\gamma \to \gamma^{-1}$ in Eq. (8). The angle of tilt for both prior and posterior ellipses are set by collision angle θ. The golden arrows depict two example critical collisions with the corresponding transitions from prior to posterior phase states. The color map (grayscale) illustrates the kinetic energy of the prior states for both the prior states themselves and the resulting posterior states. The inset: collision sketch.

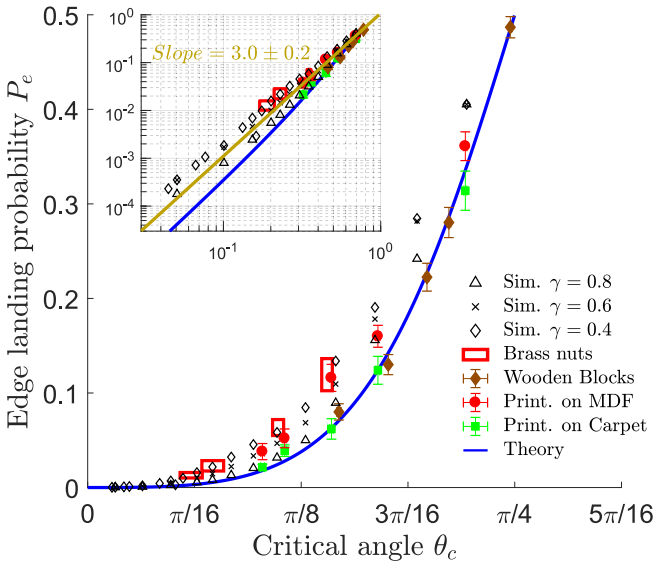

FIG. 4. Theoretical, numerical, and experimental results. Comparison of the theoretical prediction to the experimental and simulated data of two preexisting datasets. The solid symbols indicate the experimental data reported in Ref. [18] for the toss of wooden blocks and three-dimensional (3D)-printed blocks on tough carpet (brown diamonds and green squares, respectively), and printed blocks on MDF (red circles). The error bars show the binomial error. The open red rectangles depict the experimental data of Ref. [19] for the toss of brass nuts where their width and height show one standard deviation around the mean; the open black symbols (triangles, crosses, and diamonds) indicate their numerical simulations performed for distinct values of the coefficient of restitution γ with error bars smaller than symbols. The solid blue line depicts the theoretical prediction of Eq. (10), which only depends on the geometry of the coin, and through the critical angle θ_c. The inset: data in logarithmic scale; the golden (light gray) line depicts the power-law fit to all data with an exponent of 3.0 ± 0.2, consistent with the prediction of Eq. (11) for small θ_c.

A Taylor expansion of the above result for small θ_c provides the asymptotic edge landing probability,

$$P_E \sim \frac{{\theta_c}^3}{3(\pi - 2)}. \tag{11}$$

III. DISCUSSION

To test the exact solution of Eq. (10), we compare it to numerical simulations of coin tosses and experimental data for brass nuts [19] as well as to experimental data of the toss of very long cuboids [18] (see Fig. 4). Note that here coin and cuboid tossing dynamics are equivalent because the latter rotate around their longest axis only (as a 2D die [18]).

On one hand, theory neatly captures edge landing probabilities for all wooden and 3D-printed blocks (cuboids) falling on tough carpet. On the other hand, it moderately underestimates the probability for brass nuts and for blocks falling on medium density fiberboard (MDF) where they "clatter" inelastically. Lastly, coin toss simulations show that the more elastic the bouncing, the better the exact solution captures the data.

The exact model predicts no dependency of P_E on γ. However, both experiments and simulations show a moderate dependency of edge probability with the degree of inelasticity. The first assumptions in Sec. II A were experimentally validated in Ref. [19], thus, any discrepancy between data and theory should derive solely from the assumption of equiprobability of prior states, which is known to hold under air and ground friction [15].

The phase space equiprobability assumption is either grounded on random initial v and ω or grounded on the chaotic properties of the coin toss, which dominate as the number of collisions increases [15,22]. The limited initial energy in simulated tosses (to avoid "increases in computing time" [19]) greatly reduced the number of bounces, specially for low γ, hindering the chaotic nature of the process [21]. This reduced bouncing is also observed in the tosses of long cuboids on MDF but not in printed and wooden blocks on a tough carpet, "a surface on which they roll, often through many revolutions" [18]. In conclusion, the theory captures the outcome probabilities of the coin toss with arbitrarily inelastic bouncing provided that the initial velocities are random, or that the coin bounces enough times. The latter case can be

more readily achieved in a realistic setting if the bounces are more elastic.

Regarding alternative bouncing models, it is important to acknowledge the contribution of Ref. [18], who heuristically suggested that the transition probabilities from prior (supercritical) states to posterior (subcritical) states in the perfectly elastic limit might be proportional to the "activation energy", i.e., the difference between the critical energy and the lowest potential energy possible for each outcome. As proven here, the above transition probabilities are in fact proportional to the difference between the critical energy and the angle-specific minimum potential energy $mgz_{\min}(\theta)$ for any γ. Although the perfectly elastic solution proposed by Ref. [18] was, thus, inaccurate in the strict conceptual sense, it did quantitatively approximate the exact general solution of Eq. (10), and their insightful approach did point towards the right direction.

A natural follow-up for our Letter is the derivation of the optimal geometry for the fair cylindrical three-sided die. Indeed, one can constrain P_E in Eq. (10) to the fair value of one third and then solve numerically for θ_c. Thus, the predicted critical angle for the fair three-sided die is $\theta_c^{\text{fair}} \simeq 0.693$ rad; hence, the ratio of cylinder height vs diameter $\eta^{\text{fair}} := h/2r \simeq 0.831$. We note that this differs from Refs. [9,10,13] in which it was argued that $\eta \simeq 1/\sqrt{3} \simeq 0.577$ because we take bouncing into account. Our prediction is experimentally validated by the data of Ref. [18] (see Fig. 4 for $P_E \sim 1/3$), and by a recent numerical study that provides a value "close to (but not exactly equal to) $\eta \simeq 0.866$" [23]. We note that our prediction holds for either x-aligned or zero initial angular momentum (see Fig. 1) and that deviations from this constraint may effectively lower η^{fair}.

IV. CONCLUSIONS

The coin toss problem has deep implications for a broad range of modern research fields [12,15], for instance, in the study of transient chaos [24] as well as in autonomous dissipative systems, in general, for which the bouncing coin arises as a paradigmatic example. As such, the resolution of this long-standing emblematic problem opens new avenues in autonomous dissipative dynamics, whose considerations, in turn, impact the study of a wide spectrum of fields from nonequilibrium chemical reactions [25] to gravitational binary systems [26] and viscous chaotic vortices [27]. Another example of the impact of the bouncing coin problem involves quantum statistical physics [28] in which the quantum Ising chain has been shown to bear close analogies with the tossed coin. Further fields influenced by the study of the coin toss include classical and quantum chaos [24,28–30], determinism and randomness [31], fluid mechanics [27,32], ecology [33], climate dynamics [34], and hydrometeorological systems [35].

This paper presents a detailed step-by-step derivation of the long sought exact solution to the coin toss problem and, as such, this Letter provides the first analytical guideline to solve the toss of any bouncing physical object. Moreover, our combination of the phase space integral technique with the detailed description of critical collision dynamics can be generalized and applied to classical randomization mechanical systems [36] as well as to autonomous dissipative systems, in general [24,37], with direct implications to all fields mentioned in the previous paragraph.

To summarize, in this Letter we have first derived the collision equations for the bouncing coin toss grounded on standard assumptions of classical mechanics. Second, we have obtained constraints on the phase states prior and posterior to the critical collision, after which, the outcome of the toss is set. Third, we have implemented a statistical-mechanics approach by computing analytically the number of prior phase states for heads, tails, and edge outcomes. And fourth, we have derived the exact analytical outcome probabilities for the coin toss with arbitrarily inelastic bouncing. In the last section, we have validated the theoretical prediction with previous simulations and experimental data; we have discussed moderate discrepancies arising at the highly inelastic regime due to the limited number of bounces; we have highlighted the differences with previous, approximate models; we have proposed the optimal geometry for the fair cylindrical three-sided die at $h/2r \simeq 0.831$; and we have discussed the broad implications of the present results in modern physics research.

Finally, we suggest that future extensions of this Letter, including ground friction, heterogeneous mass density or additional dimensions, might provide deep insight on the landing probabilities for biased coins, as well as for the three-dimensional die throw and for the general case of an arbitrarily shaped bouncing object.

ACKNOWLEDGMENTS

We thank A. Grau Galofré, S. Hernández Navarro, and all members of the *Rashevsky Club* for interesting comments and fruitful discussions as well as acknowledge the inspiring work of D. B. Murray in the study of the coin toss problem. We declare that no funding was received for this project.

Author contributions. L.H.-N. and J.P. conceived the original idea. L.H.-N. developed the analytical model, L.H.-N. and J.P. interpreted the results. L.H.-N. and J.P. wrote the Letter.

[1] G. Galilei, Sopra le scoperte dei dadi, Opere, Firenze, Barbera **8**, 591 (1898).

[2] G. Cardano, *The Book on Games of Chance: The 16th-Century Treatise on Probability* (Courier Dover Publications, 2015).

[3] P. de Fermat and B. Pascal, *La geometría del azar: la correspondencia entre Pierre de Fermat y Blaise Pascal* (Nivola, 2007).

[4] D. T. Whiteside (ed.), *The Mathematical Papers of Isaac Newton* (Cambridge University Press, Cambridge, 1967).

[5] T. Simpson, *The Nature and Laws of Chance: Containing, Among Other Particulars, the Solutions of Several Abstruse and Important Problems* (Edward Cave, 1740).

[6] F. Budden, Throwing non-cubical dice, Math. Gazette **64**, 196 (1980).

[7] D. Singmaster, Theoretical probabilities for a cuboidal die, Math. Gazette **65**, 208 (1981).

[8] E. Heilbronner, Crooked dice, J. Recreational Math. **17**, 177 (1984).

[9] M. Parker, H. Hunt, and J. K. Rogers, How thick is a three-sided coin?, https://www.youtube.com/watch?v=-qqPKKOU-yY.
[10] P. Bosso, A. Huber, and V. Todorinov, Experimental test of fair three-sided coins, Eur. J. Phys. **42**, 025802 (2021).
[11] J. B. Keller, The probability of heads, Am. Math. Monthly **93**, 191 (1986).
[12] P. Diaconis, S. Holmes, and R. Montgomery, Dynamical bias in the coin toss, SIAM Rev. **49**, 211 (2007).
[13] E. H. Yong and L. Mahadevan, Probability, geometry, and dynamics in the toss of a thick coin, Am. J. Phys. **79**, 1195 (2011).
[14] A. Crăciun and T. O. Cheche, Modeling the unfair toss of an unbiased coin, Rom. Rep. Phys. **72**, 106 (2020).
[15] J. Strzałko, J. Grabski, A. Stefański, P. Perlikowski, and T. Kapitaniak, Dynamics of coin tossing is predictable, Phys. Rep. **469**, 59 (2008).
[16] W. Riemer, D. Stoyan, and D. Obreschkow, Cuboidal dice and gibbs distributions, Metrika **77**, 247 (2014).
[17] S. R. Kuindersma and B. S. Blais, Teaching bayesian model comparison with the three-sided coin, Am. Stat. **61**, 239 (2007).
[18] G. A. T. Pender and M. Uhrin, Predicting non-square 2d dice probabilities, Eur. J. Phys. **35**, 045028 (2014).
[19] D. B. Murray and S. W. Teare, Probability of a tossed coin landing on edge, Phys. Rev. E **48**, 2547 (1993).
[20] H. Bondi, The dropping of a cylinder, Eur. J. Phys. **14**, 136 (1993).
[21] M. Kapitaniak, J. Strzalko, J. Grabski, and T. Kapitaniak, The three-dimensional dynamics of the die throw, Chaos **22**, 047504 (2012).
[22] V. Z. Vulović and R. E. Prange, Randomness of a true coin toss, Phys. Rev. A **33**, 576 (1986).
[23] G. Subramanian, Thickness of a three-sided coin: A molecular dynamics study, Phys. Rev. E **103**, L041301 (2021).
[24] A. E. Motter, M. Gruiz, G. Károlyi, and T. Tél, Doubly Transient Chaos: Generic form of Chaos in Autonomous Dissipative Systems, Phys. Rev. Lett. **111**, 194101 (2013).
[25] S. K. Scott, B. Peng, A. S. Tomlin, and K. Showalter, Transient chaos in a closed chemical system, J. Chem. Phys. **94**, 1134 (1991).
[26] N. J. Cornish and J. Levin, Chaos and damping in the post-newtonian description of spinning compact binaries, Phys. Rev. D **68**, 024004 (2003).
[27] H. Aref, Integrable, chaotic, and turbulent vortex motion in two-dimensional flows, Annu. Rev. Fluid Mech. **15**, 345 (1983).
[28] G. Piccitto, B. Žunkovič, and A. Silva, Dynamical phase diagram of a quantum ising chain with long-range interactions, Phys. Rev. B **100**, 180402(R) (2019).
[29] J. Machicao and O. M. Bruno, Improving the pseudo-randomness properties of chaotic maps using deep-zoom, Chaos **27**, 053116 (2017).
[30] T. Dittrich, Quantum chaos and quantum randomness-paradigms of entropy production on the smallest scales, Entropy **21**, 286 (2019).
[31] K. Svozil, *Physical (A) Causality: Determinism, Randomness and Uncaused Events* (Springer, 2018).
[32] L. Heisinger, P. Newton, and E. Kanso, Coins falling in water, J. Fluid Mech. **742**, 243 (2014).
[33] D. G. Kelty-Stephen, K. Palatinus, E. Saltzman, and J. A. Dixon, A tutorial on multifractality, cascades, and interactivity for empirical time series in ecological science, Ecological Psychology **25**, 1 (2013).
[34] T. DelSole and M. K. Tippett, Predictability in a changing climate, Climate Dynamics **51**, 531 (2018).
[35] P. Dimitriadis, D. Koutsoyiannis, and K. Tzouka, Predictability in dice motion: How does it differ from hydro-meteorological processes?, Hydrological Sciences Journal **61**, 1611 (2016).
[36] J. Strzalko, J. Grabski, P. Perlikowski, A. Stefanski, and T. Kapitaniak, *Dynamics of Gambling: Origins of Randomness in Mechanical Systems*, Lecture Notes in Physics Vol. 792 (Springer, Berlin, 2009).
[37] X. Chen, T. Nishikawa, and A. E. Motter, Slim Fractals: The Geometry of Doubly Transient Chaos, Phys. Rev. X **7**, 021040 (2017).